

POOL BOILING ON MODIFIED SURFACES USING R-123

S.W. Ahmad¹, T.G. Karayiannis^{*1}, J.S. Lewis¹, R.J.M^cGlen²¹ School of Engineering and Design, Brunel University, London, UB8 3PH, UK.² Thermacore Europe Ltd, Unit 12, Wansbeck Business Park, Ashington, NE63 8QW, UK.^{*}Email: tassos.karayiannis@brunel.ac.uk

ABSTRACT

Saturated pool boiling of R-123 was investigated for five horizontal copper surfaces modified by different treatments, namely: an emery polished surface, a fine sandblasted surface, a rough sandblasted surface, an electron beam enhanced surface and a sintered surface. Each 40 mm diameter heating surface formed the upper face of an oxygen-free copper block, electrically heated by embedded cartridge heaters. The experiments were performed from the convective heat transfer regime to the critical heat flux, with both increasing and decreasing heat flux, at 1.01 bar, and additionally at 2 bar and 4 bar for the emery polished surface. Significant enhancement of heat transfer with increasing surface modification was demonstrated, particularly for the EB enhanced and sintered surfaces. The emery polished and sandblasted surface results are compared with nucleate boiling correlations and other published data.

Keywords: pool boiling, modified surfaces.

INTRODUCTION

Effect of surface modification

Surface modification is an effective passive technique for enhancing heat transfer in pool boiling applications. A variety of methods have been investigated, including emery paper or sand paper treatments, abrasive blasting, fabricated surface structures, sintered surfaces and porous coatings.

Gorenflo et al. (2004) investigated pool boiling of propane at 4.247 bar on single 8 mm OD horizontal copper tube surfaces prepared by different treatments: fine sandblasting, medium plus fine sandblasting and emery grinding and characterized by P_a values of 0.27 μm , 0.56 μm and 0.58 μm respectively. In nucleate boiling, an increase in P_a resulted in an increase in the heat transfer coefficient (at constant heat flux). A corresponding decrease of the wall superheat at transition from nucleate boiling to free convection was attributed to the increasing size of the largest surface cavities. Jones et al. (2009) examined the effect of surface roughness on pool boiling of FC-77 and water at atmospheric pressure. Ram-type electrical discharge machining (EDM) was used to prepare 25 mm x 25 mm aluminium test surfaces with average surface roughness values $R_a = 1.08 \mu\text{m}$, 2.22 μm , 5.89 μm and 10 μm . Polished surfaces with R_a values of 0.027 μm and 0.038 μm were made for comparison purposes. For FC-77, the heat transfer coefficient (at 100 kW/m²) increased continuously with

surface roughness by between 2.4 and 3 times that for a smooth surface with $R_a = 0.027 \mu\text{m}$. For water, the trend with roughness was less clear and the enhancement was between 1.5 and 1.8 times that for a smooth surface with $R_a = 0.038 \mu\text{m}$ at the same heat flux. The different behaviour for water and FC-77 was attributed to differences in the wetting characteristics of the two liquids and the cavity size distributions of the surfaces.

NOMENCLATURE

A	[m ²]	Area
a, b	[-]	Constants in equations (22)
B	[-]	Defined by equation (20)
C	[-]	Constant in equations (3,22)
c	[-]	Constant in equation (22)
c_1	[-]	Defined by equation (14)
c_p	[kJ/kg K]	Specific heat capacity
C_{sf}	[-]	Constant in equation (21)
D_b	[m]	Bubble departure diameter
d	[-]	Constant in equation (22)
F_f	[-]	Function of fluid properties, equation (5)
F_{Pr}	[-]	Function of reduced pressure, equations (5,8)
F_q	[-]	Function of heat flux, equations (5,9)
F_W	[-]	Function of heater wall, equations (5,9)
F_{WR}	[-]	Function of wall roughness, equations (9,10)
F_{WM}	[-]	Function of wall material, equations (10,11)
g	[m/s ²]	Acceleration due to gravity
h	[kW/m ² K]	Heat transfer coefficient
h_{lg}	[kJ/kg]	Specific enthalpy of vaporization
K	[-]	Variable in equations (16,17)
k	[kW/m ² K]	Thermal conductivity
M	[kg/kmol]	Molecular mass
m	[K/m]	Temperature gradient
Nu	[-]	Nusselt number
n	[-]	Exponent in equations (3,6)
P	[bar]	Pressure
P_a	[μm]	Standardized surface parameter
P_f	[1/ μm K]	Defined by equation (13)
q	[kW/m ²]	Heat flux
R	[kJ/kg K]	Specific gas constant
R_a	[μm]	Average surface roughness
$R_{p,old}$	[μm]	Surface roughness defined by DIN 4272:1960
Re_s	[-]	Modified Reynolds number

r_o	[m]	Average cavity radius
T	[K]	Temperature
U_i		Uncertainty of i^{th} component
x	[m]	Distance below the boiling surface
z	[μm]	Profile deviation from mean line
Greek Symbols		
α	[m^2/s]	Thermal diffusivity
β	[deg]	Contact angle
μ	[$\text{N s}/\text{m}^2$]	Dynamic viscosity
ν	[m^2/s]	Kinematic viscosity
ρ	[kg/m^3]	Density
σ	[N/m]	Surface tension
Subscripts		
c		Critical
g		Gas
l		Liquid
o		Reference condition
r		Reduced property
ref		Reference fluid
s		Saturation
w		Wall

Kim et al. (2008) studied the pool boiling characteristics of treated surfaces, including the effects of subcooling and surface orientation, using the dielectric liquid PF5060 and 20 mm x 20 mm copper test surfaces. Four different surfaces were tested: a plain surface, a sanded surface, a micro-finned surface and a micro-porous coated surface. The sanded surface was prepared using grade #80 sandpaper and had an average roughness height of 1.546 μm . For saturated conditions and horizontal orientation, the sanded surface achieved a wall superheat reduction of 43% at 120 kW/m^2 compared to that measured for the plain surface. McGillis et al. (1991) obtained experimental data showing the effect of surface finish on pool boiling of water at a subatmospheric pressure of 9 kPa on three flat copper surfaces. For a constant wall superheat of 25 K, the heat flux increased by about 100% when the root mean square (rms) surface roughness increased from 0.16 μm to 5.72 μm .

McGillis et al. (1991) conducted parametric experiments to determine the effects of fin geometry for low-pressure pool boiling of water on rectangular fin arrays at 9 kPa. The fin arrays were machined on 12.7 mm square copper test sections, with fin lengths from 0 to 10.2 mm, fin gaps from 0.3 mm to 3.58 mm and nominal fin widths of 1.8 mm and 3.6 mm. All the finned surfaces reduced wall superheat and extended the nucleate boiling range compared to smooth surface. However, based on the evidence for fins of 1.8 mm nominal width, additional increase in the base heat flux was fairly marginal for fin lengths greater than 2.54 mm. Smaller fin gaps were found to lead to greater heat transfer enhancement. For example, at 60 kW/m^2 , a fin gap of 0.3 mm resulted in the wall superheat decreasing by 72 % compared to a flat surface, whereas for a fin gap of 3.58 mm the decrease in wall superheat was only 28 %. No significant influence of fin width on heat transfer rates was reported.

Yu and Lu (2007) investigated the heat transfer performance of rectangular fin arrays for saturated pool boiling

of FC-72 at 1 atm. The EDM process was used to manufacture 7 x 7, 5 x 5 and 4 x 4 fin array test surfaces from copper blocks of 10 mm x 10 mm base area, with fin spacings of 0.5 mm, 1 mm and 2 mm respectively. Four different fin lengths (0.5 mm, 1 mm, 2 mm and 4 mm) were investigated and the thickness of the fins was fixed as 1 mm. In general, the heat transfer rate increased as the fin length increased and the fin spacing decreased, the maximum value being achieved with the fin array having the narrowest fin gaps (0.5 mm) and the highest fins (4 mm) was over five times that for the reference plain surface. Note that the boiling heat transfer coefficient (based on the total finned surface area) was found to be approximately independent of fin length at low heat flux. However, at moderate and high heat flux values, the heat transfer coefficient decreased as the fin length was increased at constant wall superheat.

The micro-finned surface tested by Kim et al. (2008) was fabricated by etching a copper test block to produce micro-fins of 100 μm x 100 μm square cross-section with a height of 50 μm . The spacing between the fins was 200 μm and the increase in heat transfer area was 43.6% compared to the original plain surface. Their PF5060 pool boiling curves show that for a heat flux of 120 kW/m^2 the wall superheat for the micro-finned surface was 47% lower than for a plain surface.

Surface enhancement techniques for pool boiling include porous microstructures formed by sintered metallic layers and porous coatings. Scurlock (1995) presented experimental results for saturated pool boiling of liquid nitrogen and refrigerant R-12 on surfaces with porous aluminium/silicon coatings. The surfaces were manufactured by plasma spraying a mixture of aluminium powder with 10 % silicon and polyester on to 50 mm x 50 mm aluminium plates, which were subsequently heated in air at 500°C for 2 hours to evaporate the polyester. Six surfaces were prepared with coating thicknesses between 0.13 mm and 1.32 mm. For the 0.13 mm thick coating and a heat flux of 13 kW/m^2 , the wall superheat was found to decrease compared to that for a smooth surface, by approximately 90% for LN_2 and 85% for R-12. The optimum coating thickness for maximum heat transfer coefficient was found to be 0.38 mm for LN_2 and 0.25 mm for R-12. Rainey and You (2001) investigated the effect of micro-porous coated surfaces on pool boiling of saturated FC-72 at atmospheric pressure. Copper test surfaces, 20 mm x 20 mm and 50 mm x 50 mm, were coated using a mixture of Diamond particles, Omegabond 101 and Methyl-Ethyl-Ketone (MEK), known as DOM, by drip-coating onto the 20 mm square surface and spray-coating onto the 50 mm square surface. Evaporation of the MEK produced a micro-porous layer on the surface, approximately 50 μm thick and containing 8-12 μm diamond particles. Heat transfer coefficients for nucleate boiling on the micro-porous coated surfaces were always augmented by more than 300% compared to those for plain polished surfaces. As previously mentioned, Kim et al. (2008) also tested a micro-porous coated surface for pool boiling of PF5060. The DOM coating applied to the 20 mm square copper test surface contained 4-8 μm diamond particles and was around 45 μm thick. At a heat flux of 120 kW/m^2 , the wall superheat

decreased by 66% compared to that for a plain horizontal surface.

Nucleate boiling correlations

Details of some of the correlations proposed to predict heat transfer coefficients in nucleate boiling are set out below. Stephan and Abdelsalam (1980) proposed correlations to predict the heat transfer coefficient for water, hydrocarbons, cryogenics and refrigerants in the nucleate boiling regime. The correlations were based on a regression analysis representing approximately 2800 experimental data points obtained for pool boiling on horizontal surfaces with fully established nucleate boiling under the influence of the gravity field. The pressure range for these data points was $0.0001 \leq P/P_c \leq 0.97$. The following correlation developed specifically for refrigerants with $0.003 \leq P/P_c \leq 0.78$ gave a mean absolute error of 10.6 %:

$$h = 207 \frac{k_l}{D_b} \left(\frac{q D_b}{k_l T_s} \right)^{0.745} \left(\frac{\rho_g}{\rho_l} \right)^{0.581} \left(\frac{\nu_l}{\alpha_l} \right)^{0.533} \quad (1)$$

where the bubble departure diameter D_b is expressed as

$$D_b = 0.0146 \beta \left(\frac{2\sigma}{g(\rho_l - \rho_g)} \right)^{0.5} \quad (2)$$

and the bubble contact angle β was taken as 35° for refrigerants. A mean surface roughness $R_{p,old} = 1 \mu\text{m}$ was assumed, where $R_{p,old}$ is an older roughness measure defined by the superseded standard DIN 4272:1960 and equal to $R_a/0.4$ according to Gorenflo et al. (2004). Stephan and Abdelsalam recommended that, to a first approximation, surface roughness may be accounted for by multiplying equation (1) by a factor $R_{p,old}^{0.133}$, for $0.1 \leq R_{p,old} \leq 10 \mu\text{m}$.

Cooper (1984) developed the following simple correlation for predicting the heat transfer coefficient for nucleate boiling (in $\text{W/m}^2\text{K}$) based on the reduced pressure, the heat flux (in W/m^2) and the surface roughness (in μm):

$$h = C(q)^{0.67} M^{-0.5} P_r^n (-\log_{10} P_r)^{-0.55} \quad (3)$$

and the constant was given as $C = 55$, but with the suggestion that this value should be replaced by $C = 95$ for horizontal copper cylinders. The exponent n is given by

$$n = 0.12 - 0.2 \log_{10} R_{p,old} \quad (4)$$

A comprehensive correlation for predicting pool boiling heat transfer coefficients was suggested by Gorenflo and Kenning (2009) in the form

$$\frac{h}{h_{o,ref}} = F_q F_{P_r} F_W F_f \quad (5)$$

The four factors on the right-hand side of equation (5) are functions of the heat flux, the reduced pressure, the heating surface and the fluid properties respectively, defined as

$$F_q = \left(\frac{q}{q_o} \right)^n \quad (6)$$

where $q_o = 20 \text{ kW/m}^2$ and n is given by

$$n = 0.95 - 0.3 P_r^{0.3} \quad (7)$$

$$F_{P_r} = 0.7 P_r^{0.2} + 4 P_r + \frac{1.4 P_r}{1 - P_r} \quad (8)$$

$$F_W = F_{WR} F_{WM} \quad (9)$$

where

$$F_{WR} = \left(\frac{R_a}{R_{ao}} \right)^{\frac{2}{15}} \quad (10)$$

with the reference surface roughness $R_{ao} = 0.4 \mu\text{m}$

$$F_{WM} = \left(\frac{k c_p \rho}{(k c_p \rho)_{copper}} \right)^{0.25} \quad (11)$$

and

$$F_f = \left(\frac{P_f}{P_{f,ref}} \right)^{0.6} \quad (12)$$

The fluid parameter P_f in equation (12) is defined as

$$P_f = \frac{\left(\frac{dP}{dT} \right)_s}{\sigma} \quad (13)$$

where $(dP/dT)_s$, the slope of vapour pressure curve, and σ are both at a reference pressure $P_r = 0.1$. Values of P_f , in $(\mu\text{m K})^{-1}$, are tabulated by Gorenflo and Kenning (2009) for a large number of fluids. The reference fluid values are $h_{o,ref} = 3.58 \text{ kW/m}^2\text{K}$ and $P_{f,ref} = 1.0 (\mu\text{m K})^{-1}$.

Jung et al. (2003) developed a correlation to predict pool boiling heat transfer coefficients for pure halogenated refrigerants by modifying the correlation of Stephan and Abdelsalam (1980). Based on a regression analysis of their experimental data for halogenated refrigerants, they suggested that the power on the heat flux term in equation (1) is a function of fluid properties and therefore has a unique value for each refrigerant. The new correlation is as follows:

$$h = 10 \frac{k_l}{D_b} \left(\frac{q D_b}{k_l T_s} \right)^{c_1} P_r^{0.1} (1 - T_r)^{-1.4} \left(\frac{\nu_l}{\alpha_l} \right)^{-0.25} \quad (14)$$

where

$$c_1 = 0.855 \left(\frac{\rho_g}{\rho_l} \right)^{0.309} P_r^{-0.437} \quad (15)$$

and D_b is given by equation (2). Equation (15) fitted the data of Jung et al. with a mean deviation of less than 7%.

Shekrladze (2008) presented a correlation for predicting the Nusselt number in developed nucleate boiling. The effective radius of nucleation cavities was assumed to be the characteristic linear dimension, denoted here as r_o . For commercial heating surfaces it was suggested that r_o can be

represented by an average value of 5 μm . The Shekrladze (2008) correlation is as follows:

$$\text{Nu} = \frac{hr_o}{k_l} = 0.88 \times 10^{-2} K^{0.7} \text{Re}_s^{0.25} \quad (16)$$

where

$$K = \frac{qr_o^2 \rho_g h_{lg}}{\sigma k_l T_s} \quad (17)$$

and

$$\text{Re}_s = \frac{c_p T_s \sigma \rho_l}{h_{lg}^2 \rho_g^2 \nu} \quad (18)$$

Yagov (2009) proposed a correlation on the basis of boiling fluid properties as follows:

$$q = 3.43 \times 10^{-4} \frac{k_l^2 \Delta T^3}{\nu_l \sigma T_s} \left[1 + \frac{h_{lg} \Delta T}{2RT_s^2} \right] \cdot (1 + \sqrt{1 + 800B} + 400B) \quad (19)$$

where

$$B = \frac{h_{lg} (\nu_l \rho_g)^{3/2}}{\sigma (k_l T_s)^{1/2}} \quad (20)$$

Rohsenow (1952) developed, much earlier, the following correlation for nucleate boiling of liquids other than water:

$$\frac{c_{pl} \Delta T}{h_{lg}} = C_{sf} \left[\frac{q}{h_{lg} \mu_l} \left(\frac{\sigma}{g(\rho_l - \rho_g)} \right)^{1/2} \right]^{0.33} \left[\frac{c_{pl} \mu_l}{k_l} \right]^{1.7} \quad (21)$$

Jabardo et al. (2004) reevaluated the exponents and the leading coefficient C_{sf} in the Rohsenow correlation using experimental data for refrigerants. Modified exponents were determined as 0.21 and 1.03, replacing the values 0.33 and 1.7, respectively, in equation (21). C_{sf} was expressed as a function of average surface roughness, fluid/surface material combination and reduced pressure as follows:

$$C_{sf} = C[(a \ln R_a - b)P_r - c \ln R_a + d] \quad (22)$$

For R-123 and copper the following values were found: $C = 1$, $a = 0.0077$, $b = 0.0258$, $c = 0.0036$ and $d = 0.0138$.

In this paper, experimental data are presented for saturated pool boiling of refrigerant R-123 on five different copper heating surfaces namely: emery polished, fine sandblasted, rough sandblasted, EB enhanced and sintered surfaces. The data are compared with pool boiling correlations and experimental results published in the literature.

EXPERIMENTAL SETUP

The experimental facility, shown schematically in Figure 1, consisted of the following main components: (a) the boiling chamber housing the heater block, (b) a R-123 condenser, (c) a cooling water loop and (d) a R-134a cooling unit. Electrical power supply and measurement equipment completed the experimental setup. Saturated pool boiling of R-123 was carried out in the boiling chamber. The system operated as a

two-phase thermosyphon. R-123 vapour produced in the boiling chamber was condensed in a water-cooled

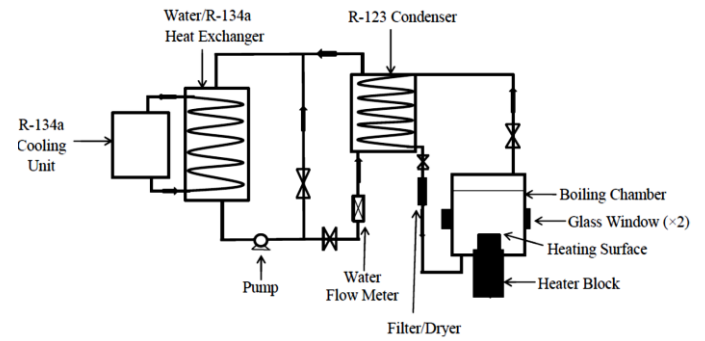


Figure 1 Schematic diagram of the experimental facility.

condenser and the condensate returned to the chamber via a filter/dryer. The cooling water used in the condenser was recirculated and chilled in a heat exchanger using a R-134a vapour compression refrigeration unit. The boiling chamber was a vertical stainless steel 304 cylinder, 220 mm in diameter and 300 mm in height. Two circular glass windows, 140 mm in diameter were mounted in the sides of the chamber in order to visualize the boiling process. Each boiling surface investigated was formed by the 40 mm upper face of a cylindrical heater block manufactured from oxygen-free copper, as illustrated in Figure 2. Six 250 W cartridge heaters were installed in the lower end of the heater block. The power supplied to the heaters was regulated using a variable transformer and measured by a power meter. Temperatures in the heater block were measured using six Type K thermocouples of 0.5 mm diameter located 5 mm, 10 mm, 15 mm, 20 mm, 25 mm and 30 mm below the boiling surface in holes 1 mm diameter and 10 mm deep. The heating block was heavily insulated by a thick PTFE sleeve. The temperature in the boiling chamber was measured by three Type K thermocouples, two placed in the liquid region and one in the vapour region.

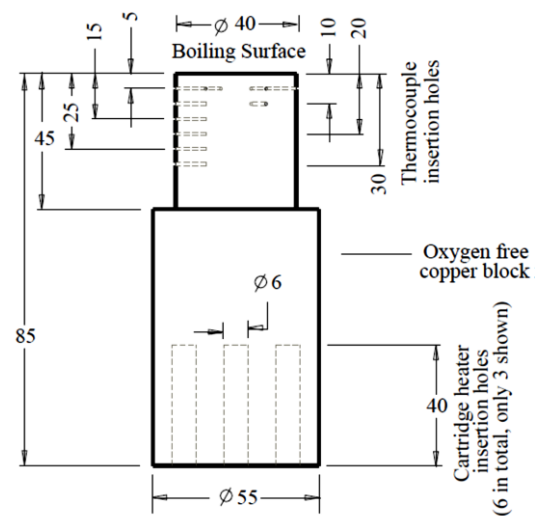


Figure 2 Schematic diagram of heater block. (All dimensions in mm)

A pressure gauge and an absolute pressure transducer were connected at the top of the chamber to monitor the pressure. To maintain saturated conditions within the chamber and to reduce heat loss an electric heater tape was wrapped around the chamber and nitrile foam rubber insulation was applied to a thickness of approximately 25 mm.

EXPERIMENTAL PROCEDURE AND DATA REDUCTION

The boiling chamber and condenser were initially filled with N₂ at 2.5 bar pressure to carry out a leakage test. Once the system was leak free, R-123 was admitted to the boiling chamber in vapour form. The refrigerant was filled to 80 mm above the boiling surface. The fluid was then boiled at a moderate heat flux for 30 minutes to remove any non-condensable gases, which were vented through a valve above the condenser. Measurements were recorded after the system reached a steady state. Tests were performed at 1.01 bar pressure for all the surfaces, for both increasing and decreasing heat flux, from the convective heat transfer regime to the critical heat flux. The effect of pressure was investigated for the emery polished surface by conducting additional tests at 2 bar and 4 bar.

The temperature gradient in the heater block and the temperature of the boiling surface were determined using the temperatures recorded at the six thermocouple positions shown in Figure 2. The heat flux was then calculated using

$$q = k_{copper} \left(\frac{dT}{dx} \right)_{x=0} \quad (23)$$

assuming heat flow in the copper block to be one-dimensional, see Ahmad et al. (2011,a). The heat transfer coefficient at the boiling surface was calculated as

$$h = \frac{k_{copper}}{(T_s - T_w)} \left(\frac{dT}{dx} \right)_{x=0} \quad (24)$$

All the thermocouples were calibrated against a precision thermometer (F250 MKII, Automatic System Laboratories) and the pressure transducer was calibrated against a dead weight tester. The uncertainty for the pressure transducer measurements was ± 0.5 kPa, and for the thermocouple measurements was ± 0.2 K. The location error of the thermocouples was estimated to be ± 0.05 mm. The propagation of uncertainties in h was determined using equation (25), see Coleman and Steele (1989).

$$\left(\frac{U_h}{h} \right)^2 = \left(\frac{U_m}{m} \right)^2 + \left(\frac{U_k}{k} \right)^2 + \left(\frac{U_{T_w}}{T_w - T_s} \right)^2 + \left(\frac{U_{T_s}}{T_w - T_s} \right)^2 \quad (25)$$

where m denotes the temperature gradient, dT/dx , in the heater block which was determined with an uncertainty of 1.6 %. A similar equation was written for the uncertainty in the heat flux, q , as follows:

$$\left(\frac{U_q}{q} \right)^2 = \left(\frac{U_k}{k} \right)^2 + \left(\frac{U_m}{m} \right)^2 \quad (26)$$

The percentage uncertainty in the heat flux was between 2 and 4 % and for heat transfer coefficient between 2.5 and 5 % for the nucleate boiling regime. All properties of R-123 were found using the EES (Engineering Equation Solver) software.

SURFACE PREPARATION AND CHARACTERIZATION

The procedures used to prepare the test surfaces are outlined below. All the surfaces were characterized using an ultrasonic stylus instrument at Kassel University as described by Luke (2006). A two-dimensional surface profile was obtained for each surface (see Figures 3 - 7). Corresponding values were reported for the surface parameter P_a , defined according to the DIN EN ISO 4287 standard the arithmetic mean deviation of the unfiltered primary profile (i.e. the surface profile without cut-off) from the mean line. In this work, P_a has been used in place of the average surface roughness R_a in evaluating correlations.

Emery polished surface

The surface was polished with emery paper P1200. It was placed on the emery paper under its own weight of 24.5 N. The block was moved on the emery paper from front to back and then sideways, 50 times in each direction. After every 50 movements the emery paper was renewed. Compressed nitrogen was then blown over the surface to remove any fine particles. A value $P_a = 0.044$ μm was reported for the emery polished surface.

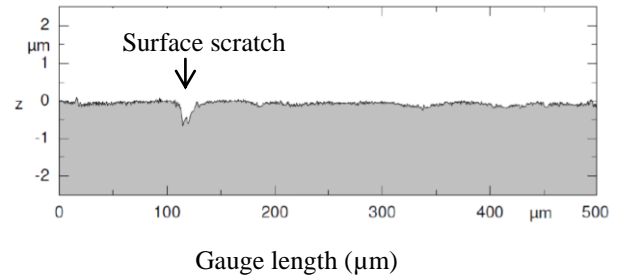


Figure 3 2-D profile for emery polished surface

Fine sandblasted surface

The surface was first carefully polished and then sandblasted with brown aluminum oxide (grit size 120-220 μm) in a standard sandblasting cabinet, as discussed in Luke (2006). During sandblasting the nozzle to surface distance was kept at 60 mm and the operating pressure was 3 bar. The P_a value was 0.0997 μm for the fine sandblasted surface.

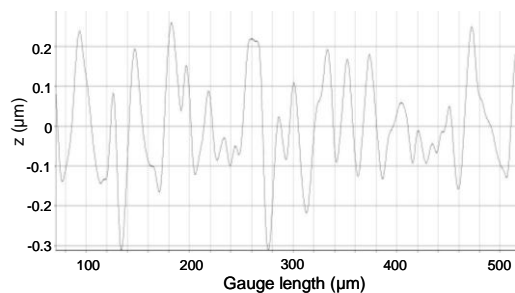


Figure 4 2-D profile for fine sandblasted surface

Rough sandblasted surface

The surface was prepared using the same procedure as used for the fine sandblasted surface, but with a coarser abrasive blasting material. Brown aluminum oxide (grit size 300-425 μm) was employed. The rough sandblasted surface was found to have a surface parameter value $P_a = 3.5 \mu\text{m}$.

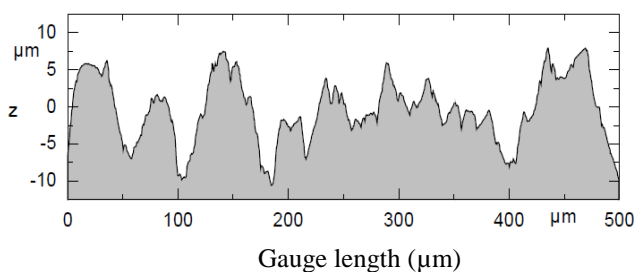


Figure 5 2-D profile for rough sandblasted surface

EB enhanced surface

The enhanced surface was prepared at TWI Cambridge using an electron beam surface modification technology known as *Surfi-Sculpt*. In this process the electron beam is moved across the surface by a programmable system causing melting and displacement of surface material to form an array of protrusions. The process is discussed in detail by Buxton et al. (2009). A value $P_a = 200 \mu\text{m}$ was determined for the EB enhanced surface.

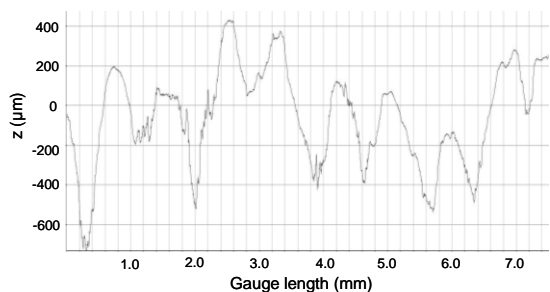


Figure 6 2-D profile for EB enhanced surface.

Sintered surface

The sintering procedure was carried out at Thermacore Europe. The sintered surface was created by sintering copper particles directly onto the upper face of the heater block. To produce the required thickness of particles a custom designed mandrel was clamped to the block, forming a chamber with a uniform depth of 0.5mm.

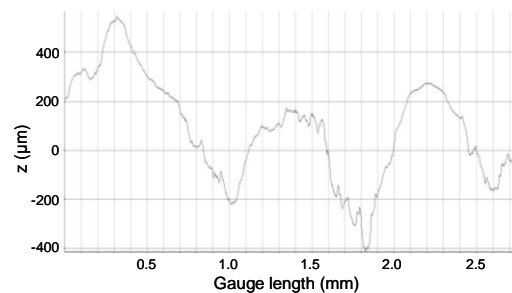


Figure 7 2-D profile for sintered surface.

Copper powder was inserted into the chamber and vibrated to ensure the particles were close packed. The assembly was heated in an inert atmosphere to just below the melting point of copper, allowing the particles to fuse together and to the surface of the heater block as a porous metal layer. To enable the material to fuse a secondary gas was used that fluxes with the powder to remove the oxide layer. A value $P_a = 144 \mu\text{m}$ was found for the sintered surface.

RESULTS AND DISCUSSION

Experimental data were collected for both increasing and decreasing heat flux for all of the surfaces tested. Hysteresis was only observed for the rough sandblasted surface and the EB enhanced surface. Due to space restrictions, only results for decreasing heat flux are presented. The repeatability of the results was routinely checked throughout the experiments. It was found that they were repeatable within the experimental error.

Effect of surface roughness

Figure 8 presents experimental data obtained in this study and earlier work by Ahmad et al. (2011,a) and Ahmad et al. (2011,b) for pool boiling of R-123 at 1 bar pressure on copper surfaces prepared using different methods; namely, emery polishing, fine and rough sandblasting, electron beam surface enhancement and sintering. The spread of the boiling curves in Figure 8 demonstrates that surface modification has an appreciable effect on the variation of heat flux with wall superheat. Experimental results reported by Zaghdoudi and Lallemand (2005) and Hristov et al. (2009) for pool boiling of R-123 at 1 bar on emery treated copper surfaces are also plotted in Figure 8 for comparison.

The results obtained for the emery polished surface with $P_a = 0.044 \mu\text{m}$ are in reasonably good agreement with the measurements of Hristov et al. (2009) who utilized an earlier version of the apparatus shown in Figure 1 at Brunel University and a boiling surface polished using P1200 emery paper followed by an ultra-fine abrasive paper. In contrast, the results of Zaghdoudi and Lallemand (2005) exhibit an earlier rise of heat flux with wall superheat for a surface prepared using No. 600 emery paper. It should be noted that No. 600 emery paper is much coarser than grade P1200 and, therefore, would be expected to produce larger cavities and deeper peak-to-valley roughness in the surface, with greater potential for bubble formation at lower wall superheats. Beyond this, it is difficult to compare the emery polished surface results obtained by the

present authors and Hristov et al. (2009) and those of Zaghoudi and Lallemand (2005) because surface roughness was not quantified in the latter two studies.

The experimental results shown in Figure 8 for the two sandblasted boiling surfaces are characterized by different values of the standardized surface parameter: $P_a = 0.099 \mu\text{m}$ for the fine sandblasted surface and $P_a = 3.5 \mu\text{m}$ for the rough sandblasted surface. As heat flux and wall superheat increase, the fine sandblasted surface data are initially in-line with the curve for the emery polished surface when natural convection is the principal heat transfer mode. At a wall superheat slightly above 12 K the fine sandblasted results diverge sharply upward with the onset of nucleate boiling. This enhancement of boiling heat transfer is consistent with the presence of larger cavities on the rougher surface; i.e. $P_a = 0.099 \mu\text{m}$ compared to $0.044 \mu\text{m}$ for the polished surface. It should be mentioned that the roughness value reported here for the emery polished surface may be slightly high due to surface scratches within the gauge length over which P_a was evaluated, as indicated in Figure 3.

In the case of the rough sandblasted surface ($P_a = 3.5 \mu\text{m}$) the boiling curve is further shifted to the left in Figure 8, compared with the curves for the fine sandblasted and emery polished surfaces. This pattern illustrates a progressive decrease, with increase of the surface roughness, of the wall superheat needed to dissipate a given heat flux by nucleate pool boiling on these surfaces. Inspection of the two-dimensional surface profiles in Figures 4 and 5 shows that the microstructure of the rough sandblasted test surface had much deeper valleys, higher peaks and a wider distribution of cavity sizes than the fine sandblasted test surface. Hence, the rough sandblasted surface microstructure would be more effective, both in a vapour trapping role and in promoting bubble formation over a range of wall superheats.

The EB enhanced surface and the sintered surface both achieved a large improvement in heat transfer compared to the conventional emery polished and sandblasted surfaces, as evidenced by their much steeper boiling curves in Figure 8. Application of the EB surface modification process causes the growth of a pattern of protrusions above the original surface level, accompanied by associated cavities in the substrate. This macrostructure is reflected by the large value of the standardized surface parameter, $P_a = 200 \mu\text{m}$, measured for the EB enhanced surface, significantly larger than the P_a values determined for the other surfaces tested. The effectiveness of the cavities formed by the EB surface enhancement technique in trapping vapour is believed to be the primary reason for the large observed augmentation of heat transfer in nucleate boiling.

In addition, the increase in the heat transfer surface area provided by the protrusions may be a secondary factor contributing to an increase in the base heat flux. The strongest influence of surface modification on pool boiling heat transfer is displayed by the sintered surface results shown in Figure 8, albeit the surface $P_a = 144 \mu\text{m}$ was smaller than for the EB enhanced surface. The sintering process forms a porous metallic (copper) structure on the heater block surface of assumed uniform porosity and cavity distribution, providing

vapour entrapment volume and a large number of active nucleation sites.

The heat transfer coefficient augmentation can be expressed as the ratio $h_{\text{modified surface}}/h_{\text{polished surface}}$. Trend lines of this factor are compared in Figure 9 for heat fluxes up to 220 kW/m^2 . For the sintered, EB enhanced, rough sandblasted and fine sandblasted test surfaces the heat transfer coefficients were found to be augmented by around 9, 6.5, 2 and 1.5 times the value for the emery polished surface, respectively.

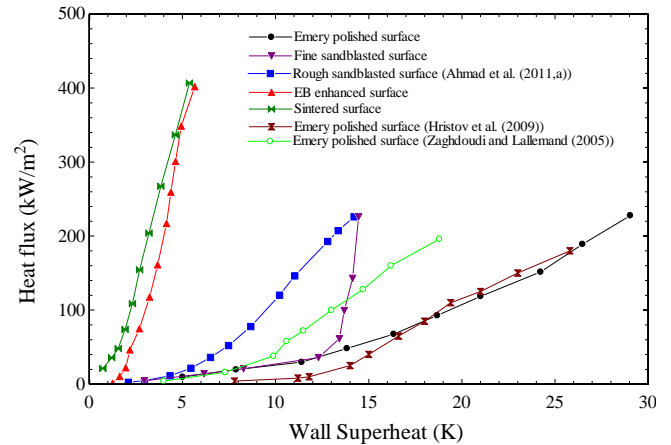


Figure 8 Boiling curves for modified surfaces, at $P = 1.01$ bar.

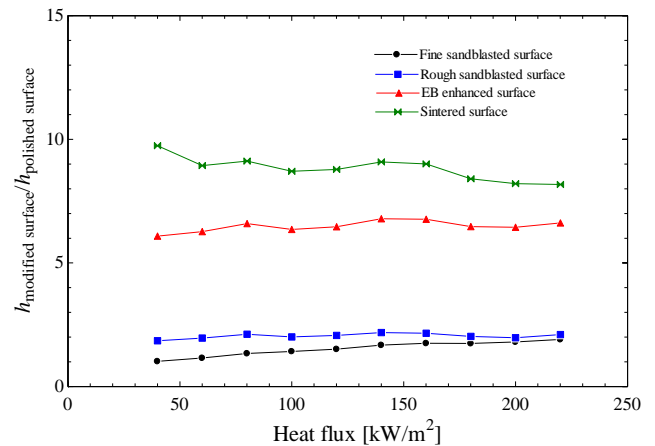


Figure 9 Augmentation of heat transfer coefficient due to surface modification

Comparison with correlations

Experimental heat transfer coefficients obtained in this study for pool boiling of R-123 on the emery polished surface, at pressures of 1.01 bar, 2 bar and 4 bar, are compared with predictions based on published nucleate boiling correlations in Figures 10, 11 and 12, respectively. Similar comparisons are presented in Figures 13 and 14 for the results obtained at 1.01 bar with the fine sandblasted surface and the rough sandblasted surface, respectively. These surfaces cover a range of roughness with standardized surface parameter values $P_a = 0.044 \mu\text{m}$ (emery polished), $P_a = 0.099 \mu\text{m}$ (fine sandblasted) and $P_a = 3.5 \mu\text{m}$ (rough sandblasted). As previously mentioned, P_a values were substituted for the average surface roughness R_a in prediction calculations, although it is noted that the

roughness of the heater surface is not used in all of the correlation equations considered here.

The correlation proposed by Stephan and Abdelsalam (1980) for refrigerants, given by equation (1), is based on a regression analysis of published data covering a wide range of reduced pressure and includes thermal, transport and wetting properties of the fluid. An average surface roughness $R_{p,old} = 1 \mu\text{m}$ was assumed in the development of this correlation. It was suggested that equation (1) should be multiplied by $R_{p,old}^{0.133}$ to account for the influence of surface roughness values other than $1 \mu\text{m}$. When this factor is applied with the Stephan-Abdelsalam correlation, as plotted in Figure 10, the calculated heat transfer coefficients under predict the experimental results for the emery polished surface at $P = 1.01$ bar, only falling within the $\pm 20\%$ error band at higher heat fluxes. If the surface roughness factor is not included, the predictions (not shown) are within $\pm 20\%$ of the experimental data in the mid-to-low heat flux range, but are too high at high heat fluxes and too low at low heat fluxes. In the simple correlation developed by Cooper (1984), the properties of the boiling fluid are represented in terms of the reduced pressure P_r and the molecular mass M only. The heater surface roughness measure $R_{p,old}$ is included in an exponent on P_r . The Cooper correlation predicted line in Figure 10, calculated using equation (3) with $C = 95$, exhibits slightly closer agreement with the $P = 1.01$ bar experimental results than that of the Stephan-Abdelsalam correlation and remains within the $\pm 20\%$ error band apart from at the lowest heat flux values. The Jung et al. (2003) correlation for halogenated refrigerants is a modified form of the Stephan and Abdelsalam (1980) correlation and, following Cooper (1984), introduces the reduced properties P_r and T_r . However, their equation does not include any term to account for the heater surface condition. Predicted values calculated with the Jung et al. correlation are within $\pm 20\%$ of the polished surface experimental data for $P = 1.01$ bar, except at the extremes of the heat flux range.

Heat transfer coefficients predicted from the correlations and the experimental results for the emery polished surface, at test pressures of 2 bar and 4 bar, are compared in Figures 11 and 12 respectively. It is immediately evident that the correlations discussed above, due to Stephan and Abdelsalam (1980), Cooper (1984) and Jung et al. (2003), show better agreement with the higher pressure data, particularly at $P = 2$ bar, than was obtained for the 1.01 bar condition. The heat transfer prediction equation developed by Yagov (2009) is based on an approximate theoretical model of nucleate boiling and includes empirically determined constants and the boiling fluid properties. Predictions made with this equation show close agreement with the experimental data for the emery polished surface for 1.01 bar and 2 bar, but slightly less good agreement at 4 bar; see Figures 10, 11 and 12.

The calculation method of Gorenflo and Kenning (2009) involves non-dimensional functions representing the relative influences of heat flux, reduced pressure, fluid properties and heating surface roughness and material properties on the heat transfer coefficient relative to that for a fictitious reference fluid. For $P = 1.01$ bar, the predicted coefficients are within the

range of values given by the other correlations, as shown in Figure 10. However, at 2 bar and 4 bar, the predicted values only agree at low heat fluxes, but then deviate increasingly as the heat flux increases, as can be seen in Figures 11 and 12. This behaviour is presently unexplained and requires further investigation.

Shekrladze (2008) developed a nucleate boiling correlation with the average effective radius at the mouth of nucleation cavities as the characteristic linear size. As mentioned earlier, Shekrladze (2008) suggested using a value $r_o = 5 \mu\text{m}$ as typical of commercial surfaces. Since r_o was unknown for the emery polished and sandblasted surfaces tested in this work, a constant value of $5 \mu\text{m}$ was used in order to evaluate equation (16). Nevertheless, the predicted heat transfer coefficients are mostly within $\pm 20\%$ of the experimental results for the emery polished surface at all pressures, except at low heat fluxes.

Jabardo et al. (2004) employed curve fits of experimental data for refrigerants (including R-123) to modify the exponents and the surface-fluid coefficient C_{sf} in the original Rohsenow (1952) nucleate boiling correlation. An expression, equation (22), was developed for calculating C_{sf} as a function of surface roughness and reduced pressure. Predictions made using the modified correlation are comparable with those of the Stephan and Abdelsalam (1980) correlation (including the surface roughness factor).

Figures 10-12, and the discussion above, relate to the emery polished surface characterized by the single P_a value of $0.044 \mu\text{m}$. It is of interest to examine how the same correlations perform in predicting heat transfer coefficients for the fine and rough sandblasted surfaces. The predictions from the Jung et al. (2003), Yagov (2009) and Shekrladze (2008) correlations for the sandblasted surfaces shown in Figures 13 and 14 are identical to those for the emery polished surface shown in Figure 10. This is because the conditions (saturated, $P = 1.01$ bar), and hence fluid properties, were the same in all cases and because surface roughness does not appear in these correlations. Also, a constant value of r_o was assumed in the Shekrladze correlation.

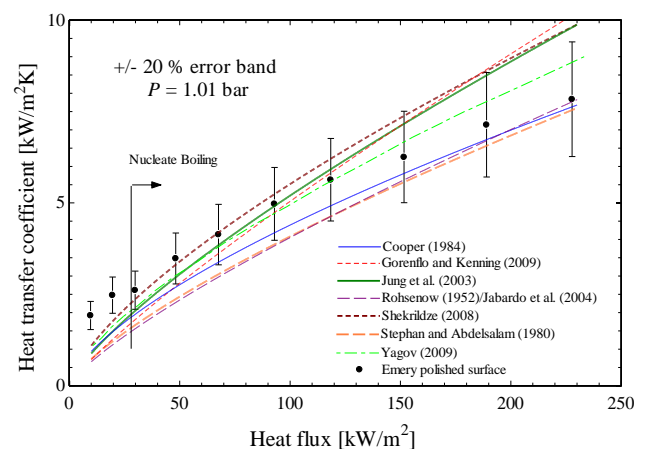


Figure 10 Comparison of pool boiling results of emery polished surface with published correlations, at $P = 1.01$ bar

In the case of the fine sandblasted surface (see Figure 13), all the predictions fall below the experimental data. In Figure 9, the heat transfer coefficient augmentation for the fine sandblasted surface was around 1.5 times that of the emery polished surface, for an increase in P_a from 0.044 μm to 0.099 μm , whereas the dependence of h on surface roughness in the Stephan-Abdelsalam and Gorenflo-Kenning equations follows a weaker $h \propto R_a^{4/15}$ relationship. Furthermore, it is known that sandblasted surfaces have a uniform granular microstructure with a larger size distribution of cavities, or roughness range, than produced by emery grinding; see Luke (2009). Consequently, the use of R_a alone may not be adequate to fully represent the surface condition.

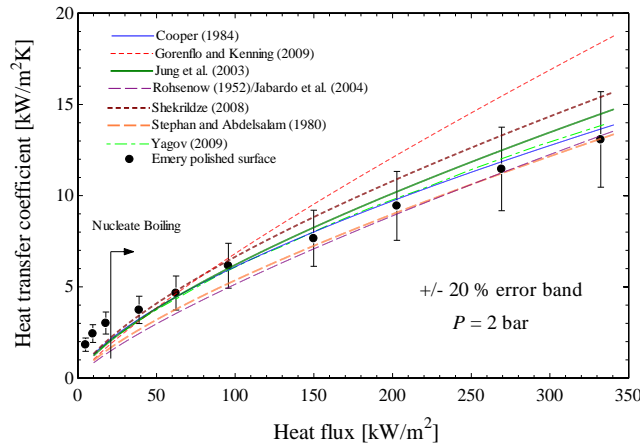


Figure 11 Comparison of pool boiling results of emery polished surface with published correlations, at $P = 2$ bar.

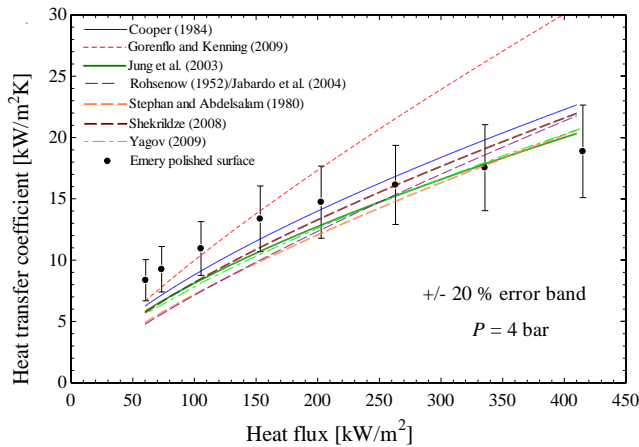


Figure 12 Comparison of pool boiling results of emery polished surface with published correlations, at $P = 4$ bar.

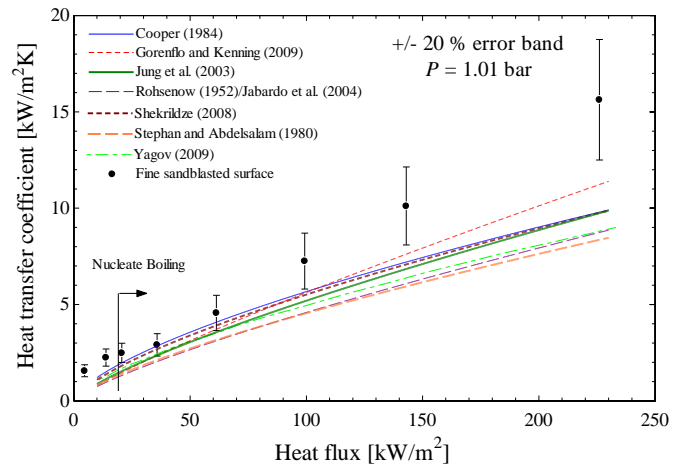


Figure 13 Comparison of pool boiling results of fine sandblasted surface with published correlations, at $P = 1.01$ bar.

The comparison for the rough sandblasted surface ($P_a = 3.5 \mu\text{m}$) in Figure 14 shows large deviations between the predictions and the experimental data, as expected, except for the Jabardo et al. (2004) modification of the Rohsenow (1952) correlation and the Gorenflo and Kenning (2009) correlation.

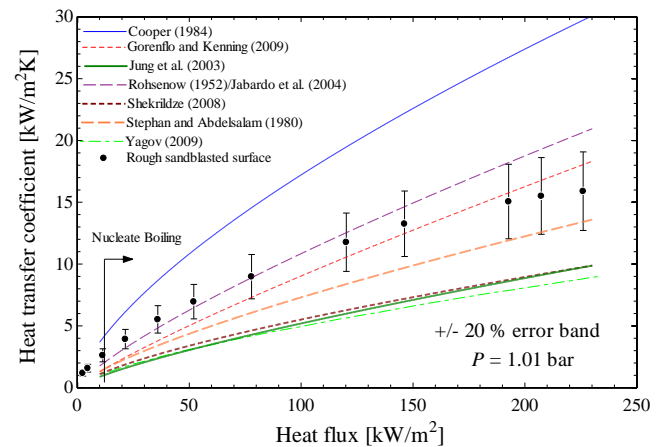


Figure 14 Comparison of pool boiling results of rough sandblasted surface with published correlations, $P = 1.01$ bar.

CONCLUSIONS

The effects of heater surface modifications on pool boiling in saturated R-123 were investigated experimentally. Boiling curves were established for emery polished, sandblasted, electron beam enhanced and sintered surfaces. The following conclusions can be drawn:

- (1) Surface modification can yield significant enhancement of the heat transfer coefficient. The best performance was achieved by the sintered surface with a heat transfer coefficient approximately nine times that for the emery polished surface. The corresponding augmentation factors for the EB enhanced, fine sandblasted and rough sandblasted surfaces were around 6.5, 2 and 1.5 respectively.

- (2) The experimental heat transfer coefficients for the emery polished surface (at 1.01 bar, 2 bar and 4 bar) were compared with predictions from seven different nucleate boiling correlations. Some correlations gave predictions within $\pm 20\%$ of the experimental results over wide ranges of heat flux and pressures. Comparison of experimental and predicted coefficients for the sandblasted surfaces (at 1.01 bar) showed much greater disagreement, with general under-prediction for the fine sandblasted surface and some large deviations for the rough sandblasted surface.
- (3) The pool boiling results obtained for the emery polished surface and two sandblasted surfaces suggest that the effect of different heater surface conditions may not be adequately represented by the dependence of heat transfer coefficient on average surface roughness R_a assumed in the nucleate boiling correlations.

Acknowledgements

The first author was supported by the Government of Pakistan under a scholarship program. The technical support of Prof. A. Luke of Kassel University and Dr. A.L. Buxton of TWI Cambridge is also acknowledged.

REFERENCES

- Ahmad, S. W., Karayiannis, T. G., Kenning, D. B. R. and Luke, A. (2011,a). "Compound effect of EHD and surface roughness in pool boiling and CHF with R-123." Applied Thermal Engineering **31**: 1994-2003.
- Ahmad, S. W., Karayiannis, T. G., Lewis, J. S., McGlen, R. J. and Kenning, D. B. R. (2011,b). Pool boiling on an enhanced surface with EHD. 12th UK National Heat Transfer Conference, Leeds, UK.
- Buxton, A. L., Ferhati, A., Glen, R. J. M., Dance, B. G. I., Mullen, D. and Karayiannis, T. G. (2009). EB surface engineering for high performance heat exchangers. First International electron beam welding conference Chicago USA.
- Coleman, W. H. and Steele, G. W. (1989). Experimentation and Uncertainty Analysis for Engineers, John Wiley & Sons.
- Cooper, M. G. (1984). "Saturation nucleate pool boiling – a simple correlation." ICHEME Symposium Series **86**: 786-793.
- Gorenflo, D., Chandra, U., Kottoff, S. and Luke, A. (2004). "Influence of thermophysical properties on pool boiling of refrigerants." International Journal of Refrigeration **27**: 492-502.
- Gorenflo, D. and Kenning, D. B. R. (2009). H2 Pool boiling, VDI Heat Atlas Springer-Verlag.
- Hristov, Y., Zhao, D., Kenning, D. B. R., Sefiane, K. and Karayiannis, T. G. (2009). "A study of nucleate boiling and critical heat flux with EHD enhancement." Heat Mass Transfer **45**: 999-1017.
- Jabardo, J. M. S., Silva, E. F. D., Ribatski, G. and Barros, S. F. D. (2004). "Evaluation of the Rohsenow correlation through experimental pool boiling of halocarbon refrigerants on cylindrical surfaces." J Braz. Soc. of Mech Sci Eng **24**: 218-230.
- Jones, B. J., McHale, J. P. and Garimella, S. V. (2009). "The influence of surface roughness on nucleate pool boiling heat transfer." Journal of Heat Transfer **131**: 1-14.
- Jung, D., Kim, Y., Ko, Y. and Song, K. (2003). "Nucleate boiling heat transfer coefficients of pure halogenated refrigerants." International Journal of Refrigeration **26**: 240-248.
- Kim, Y. H., Lee, K. J. and Han, D. (2008). "Pool boiling enhancement with surface treatments." Heat Mass Transfer **45**: 55-60.
- Luke, A. (2006). "Preparation, measurement and analysis of microstructure of evaporator surfaces." International Journal of Thermal Sciences **45**(237-256).
- Luke, A. (2009). "Preparation and analysis of different roughness structures for evaporator tubes." Heat Mass Transfer **45**: 909-917.
- McGillis, W. R., Carey, V. P., Fitch, J. S. and Hamburg, W. R. (1991). "Pool boiling enhancement techniques for water at low pressure." Seventh IEEE Semi-Therm Symposium: 64-72.
- Rainey, K. N. and You, S. M. (2001). "Effects of heater size and orientation in pool boiling heat transfer from micro porous coated surfaces." International Journal of Heat and Mass Transfer **44**: 2589-2599.
- Rohsenow, W. M. (1952). "A method of correlating heat transfer data for surface boiling liquids." Journal of Heat Transfer **74**: 969-976.
- Scurlock, R. G. (1995). "Enhanced boiling heat transfer surfaces." Cryogenics **35**: 233-237.
- Shekrladze, I. G. (2008). "Boiling Heat Transfer: Mechanisms, Models, Correlations and the lines of further research." The Open Mechanical Engineering Journal **2**: 104-127.
- Stephan, K. and Abdelsalam, M. (1980). "Heat transfer correlation for natural convection boiling." International Journal Heat and Mass Transfer **23**: 73-87.
- Yagov, V. V. (2009). "Nucleate boiling heat transfer: possibilities and limitations of theoretical analysis." Heat Mass Transfer **45**: 881-892.
- Yu, C. K. and Lu, D. C. (2007). "Pool boiling heat transfer on horizontal rectangular fin array in saturated FC-72." International Journal of Heat and Mass Transfer **50**: 3624-3637.
- Zaghdoudi, M. C. and Lallemand, M. (2005). "Pool boiling heat transfer enhancement by means of high DC electric field." The Arabian Journal for Science and Engineering **30**: 189-212.